7-2022

Lab-scale Data and Microbial Community Structure Suggest Shortcut Nitrogen Removal as the Predominant Nitrogen Removal Mechanism in Post-Aerobic Digestion (PAD)

Fabrizio Sabba
Black & Veatch

Patrick J. McNamara
Marquette University, patrick.mcnamara@marquette.edu

Eric Redmond
Black & Veatch

Mike Young
Trinity River Authority of Texas

Leon Downing
Black & Veatch

Water Environment Research, Vol. 94, No. 7 (July 2022): e10762. DOI.

Lab-Scale Data and Microbial Community Structure Suggest Shortcut Nitrogen Removal as The Predominant Nitrogen Removal Mechanism in Post-Aerobic Digestion (PAD)

Fabrizio Sabba
Black & Veatch, Overland Park, Kansas
Patrick McNamara
Black & Veatch, Overland Park, Kansas
Department of Civil, Construction and Environmental Engineering, Marquette University, Milwaukee, Wisconsin
Eric Redmond
Black & Veatch, Overland Park, Kansas
Caitlin Ruff
Black & Veatch, Overland Park, Kansas
Mike Young
Trinity River Authority of Texas, Arlington, Texas,
Leon Downing

Black & Veatch, Overland Park, Kansas

Abstract

Implementing an aerobic digestion step after anaerobic digestion, referred to as “post aerobic digestion” (PAD), can remove ammonia without the need for an external carbon source and destroy volatile solids. While this process has been documented at the lab-scale and full-scale, the mechanism for N removal and the corresponding microbial community that carries out this process have not been established. This research gap is important to fill because the nitrogen removal pathway has implications on aeration requirements and carbon demand, that is, short-cut N-removal requires less oxygen and carbon than simultaneous nitrification–denitrification. The aims of this research were to (i) determine if nitrite (NO_2^-) or nitrate (NO_3^-) dominates following ammonia removal and (ii) characterize the microbial community from PAD reactors. Here, lab-scale PAD reactors were seeded with biomass from two different full-scale PAD reactors. The lab-scale reactors were fed with biomass from full-scale reactors and operated in batch mode to quantify nitrogen species concentrations (ammonia, NH_4^+, NO_2^-, and NO_3^-) over time. Experimental results revealed that NO_2^- production rates were several orders of magnitude greater than NO_3^- production rates. Indeed, nitrite accumulation rate (NAR) was greater than 90% at most temperatures, confirming that shortcut nitrogen removal was the dominant NH_4^+ removal mechanism in PAD. Microbial community analysis via 16S rRNA sequencing indicated that ammonia oxidizing bacteria (AOB) were much more abundant than nitrite oxidizing bacteria (NOB). Overall, this study suggests that aeration requirements for post-aerobic digestion should be based on NO_2^- shunt and not complete simultaneous nitrification denitrification.

Practitioner Points

- AOB are a key feature of PAD microbial communities
- NOB are present, but in much lower abundance than AOB
- High nitrite accumulation ratio suggests shortcut nitrite as the main mechanism for nitrogen removal
- Nitritation in PAD reactors is sustained at temperatures as high as 40°C
- No ammonia oxidation occurred at 50°C implying different mechanisms of nitrogen removal including ammonia stripping

INTRODUCTION

Eutrophication is detrimental to water quality and occurs when excess nutrients (N, P) enter receiving water bodies (Zheng et al., **2018**). Wastewater treatment plants (WWTPs), a.k.a. Water Resource Recovery Facilities (WRRFs), have been targeted by regulators as a discharge source of nutrients that can be managed to reduce nutrient loads into watersheds. These pressures from regulators, along with the recent push to use WRRFs for resource recovery, including water, energy, carbon, and nutrients (Mannina et al., **2021**), has led to progress in nutrient removal technologies (Liu et al., **2020**; Venkiteshwaran et al., **2018**).

Nitrification and denitrification are two essential processes used during biological nitrogen removal (BNR) in WRRFs (Delgado Vela et al., **2015**). Nitrification is a two-step process performed by ammonia oxidizing bacteria (AOB) and nitrite oxidizing bacteria (NOB) whereby ammonia (NH_4^+) is first oxidized

to nitrite (NO_2^-) and then nitrate (NO_3^-). Oxygen is required for both steps and serves as the electron acceptor. During denitrification, heterotrophic denitrifying bacteria reduce NO_3^- to nitrogen gas (N_2) via intermediates that include NO_2^-, nitric oxide (NO) and nitrous oxide (N_2O) (Sabba et al., **2018**). No oxygen is required because NO_3^- serves as the electron acceptor, but external carbon sources are often needed to serve as the electron donor to meet discharge limits. BNR processes including nitrification and denitrification are considered advantageous when compared to physicochemical processes for wastewater treatment because they are more cost-effective (Rahimi et al., **2020**).

To reduce energetic operating costs several novel BNR technologies have been developed in the last 20 years. Examples include simultaneous nitrification denitrification (SND) (Chen et al., **2015**; Iannacone et al., **2020**), shortcut nitrification and denitrification (Roots et al., **2020**), and complete autotrophic nitrogen removal over nitrite (CANON) (Vázquez-Padín et al., **2011**). Novel reactor configurations exploiting novel bacterial and metabolic discoveries have also furthered our understanding of nitrogen cycling. This is the case for, for example, complete ammonia oxidation, comammox, and anaerobic ammonia oxidation, anammox (Kuenen, **2008**; Roots et al., **2019**; van Kessel et al., **2015**) processes: the former able to carry out nitrification in a single step from NH_4^+ to NO_3^- and the latter able to remove NH_4^+ in presence of NO_2^- and in absence of oxygen (Kuenen, **2008**; Roots et al., **2019**; van Kessel et al., **2015**). All these processes are nutrient removal processes typically applicable to liquid streams. However, solids streams also carry high nutrient loads (Carey et al., **2016**).

Nutrients from solids streams are often returned to the head of a WRRF in filtrate streams following thickening and dewatering (Carey et al., **2015**). Nutrient removal processes for solids streams have not been a major focus in research or practice. Anaerobic processes such as anaerobic digestion do not remove nutrients. Physical processes such as adsorption do not work well with thick streams such as biosolids (Tong et al., **2016**, **2017**). An aerobic digestion phase after anaerobic digestion, referred to as post-aerobic digestion (PAD), has received more attention as a nutrient removal process that can be applied to solids streams (Kim & Novak, **2011**; Parravicini et al., **2008**; Zupančič & Roš, **2008**).

PAD is primarily of interest as an NH_4^+ removal process. Anaerobic digestion often yields elevated levels of NH_4^+, and PAD has been shown to remove NH_4^+. A unique feature of PAD, compared to nutrient removal processes typically used in liquid streams described above, is that no external carbon source is required because of the available carbon content leaving the anaerobic digester (Bauer et al., **2016**). For PAD reactors to operate, no external inputs are needed other than the effluent biosolids from the anaerobic digester (McNamara et al., **2022**). The process uses aeration, but the aerobic microbes do not have sufficient carbon to increase their biomass similarly to activated sludge; therefore, they undergo endogenous decay, and there is typically some volatile solids removal (VSR, ~10%) (Ahmad et al., **2016**; Kim & Novak, **2011**). There is increased attention towards achieving increased VSR; this can happen by using free ammonia (FA) (Wei et al., **2018**) or free nitrous acid (FNA) (Wang et al., **2016**) to pretreat sludge from the anaerobic digester prior to PAD processing. In addition to chemical pretreatment, physical treatment of anaerobically digested sludge, for example, ultrasounds, has also shown promising results for solids removal (Song et al., **2017**).

Different lab-scale studies postulated that PAD reactors, given their propensity to remove nitrogen and the dissolved oxygen variation across the reactors, are based on a biological process that involves simultaneous nitrification denitrification (SND) (Ahmad et al., **2016**; Kumar et al., **2006**; Tomei et

al., **2011**). Constant aeration and intermittent aeration have been shown to be successful. Shortcut nitrogen removal could be the nitrogen removal mechanism based on the presence of NO_2^-. Some research previously used the term SND but was not able to verify if shortcut nitrogen removal was occurring (Tomei et al., **2016**). Due to the lower oxygen demand of shortcut N removal compared to SND, it is important to understand the nitrogen removal mechanism. For example, understanding whether nitrogen is removed via full nitrification or nitritation would be a key finding that can translate into conspicuous economical savings for aeration strategies (Daigger, **2014**).

McNamara et al. (**2022**) described two full-scale operated PAD reactors at MWR Denver and Boulder WTF and found that nitrogen loading rate, SRT, and pH can be important operational parameters for a healthy operation of PAD systems. While this study furthered our knowledge and provided extensive information about operational strategies that complements previous lab-scale studies, no research has been conducted on the microbial community that drives the biological processes in PAD nor has there been specific rate studies investigating NO_3^- and NO_2^- production concomitant with microbial community sequencing. The main goal of this research was to determine the nitrogen removal pathway in PAD and characterize the microbial community that drives this N removal process. We hypothesized that NO_2^- would form to a greater extent than NO_3^- and that AOB would be more prevalent than NOB. We operated two different lab-scale reactors seeded with biomass from two different full-scale PAD reactors. NH_4^+ removal, NO_2^- production, and NO_3^- production were assessed across different temperatures and alkalinity. Biomass composition evaluated via 16S Illumina sequencing to identify the important microbes for nitrogen removal during PAD operation.

MATERIAL AND METHODS

Lab-scale PAD reactors for batch experiments

Biomass samples were obtained from full-scale PAD reactors operating at Boulder Wastewater Treatment Facility (WTF) and the Denver Metro Water Recovery Northern Treatment Plant (MWR NTP). Denver's PAD installation occurred in 2016, and Denver's installation occurred in 2017. The two PADs reactors are characterized by different process operations where Denver's PAD reactor is supplemented with calcium hydroxide (lime) for added alkalinity and phosphorus precipitation, while alkalinity addition is not necessary at Boulder. Specifically, Boulder is operated with an average 11.9-day solids retention time (SRT) and an average ammonia loading rate of 0.18 KgN m^{-3} day^{-1}, while Denver uses an average 17.1-day SRT and an average ammonia loading rate of 0.098 KgN m^{-3} day^{-1}. Further details about sizing, process, and operation can be found in McNamara et al. (**2022**).

The biomass from each full-scale PAD reactor was used to seed the lab-scale experiments. Biomass was collected from full-scale PAD reactors, stored in plastic bottles at 4°C, and shipped in coolers to the Trinity River Authority of Texas (TRA) Central Regional Wastewater System (CRWS) treatment plant for testing.

Lab-scale batch tests were performed in two 2-L glass cylindrical beaker with an active volume of 1 L. For each batch test, 1 L of biomass (i.e., effluent) from a full-scale PAD reactor (Denver or Boulder wastewater treatment plant) was fed ammonium chloride (NH_4Cl) with an initial concentration of 1,000 mg L^{-1} to test for maximum nitrification rates. The batch reactors were operated with two varying parameters: temperature and alkalinity, to understand their impacts on nitrification and the

main nitrogen removal mechanisms. Reactors filled with biomass from Boulder are referred to PAD test B and Reactors filled with biomass from Denver are referred to as PAD test D. A schematic of the reactors' setup can be found in Figure **1**. Biomass from both plants was preserved at 4°C for up to a week and warmed up/acclimated to testing temperature in a water bath before beginning batch tests. Excess biomass was disposed of at the end of the week, and a new shipment of biomass from both treatment facilities was received for a fresh batch each week of testing.

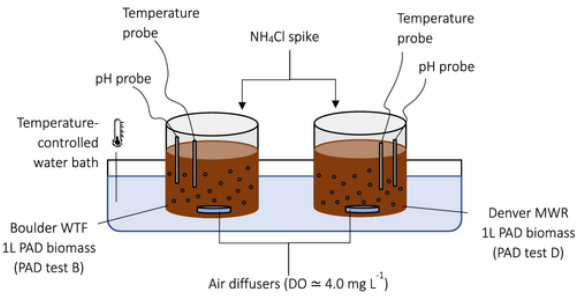

FIGURE 1 Batch tests experimental setup for nitrification rate testing

The first set of experiments focused on the impact of temperature on nitrification rates. At beginning of the temperature tests, NH_4Cl was spiked to achieve 600 mgN L^{-1}; each batch test ran for approximately 5 h from the time they were spiked. Samples were collected at 30-min intervals for a total of 11 samples, including an initial time point, t_0. All the parameters were tracked following procedure and standard methods reported in Table **1**.

TABLE 1. Analytical method, kit, or probe used to collect data for both reactors

Parameter	**Method/probe used**
Total solids	Standard method
Volatile solids	Standard method
Ammonia	Hach DR6000
Nitrite	Hach DR6000
Nitrate	Hach DR6000
Orthophosphate	Hach DR6000
pH	Orion Star A211 probe
TIC	Standard method
Dissolved oxygen	Hach HQ40d

The biomass from each plant was kinetically characterized for nitrification with batch kinetic tests performed at different set temperatures (24.5°C, 30°C, 40°C, and 50°C). Normal operating temperature is between 30°C and 40°C (McNamara et al., **2022**), while 50°C was selected as an extreme boundary condition. The temperature was controlled via a thermostatic bath. Dissolved oxygen was kept at saturation by constant sparging via compressed air at a flow rate suitable to support the DO at a set-point of 4 mg L^{-1}. In McNamara et al. (**2022**), full-scale PAD reactors were operated at low DO to achieve full nitrogen removal via SND or nitritation/denitritation, while here, full-saturation and constant DO was supplied to establish maximum accumulation rates of NO_2^- or NO_3^-.

The second set of experiments focused on the impact of alkalinity on nitrification. These tests were conducted in a water bath at a constant temperature of 30°C. The general setup of the test was identical to the temperature test; however, to track the consumption of alkalinity, pH was constantly monitored with a pH-meter (Orion Star A211 probe). Alkalinity adjustment, in the form of sodium hydroxide (NaOH), was initially based on the alkalinity required for 200 mg N L^{-1} of NH_4^+ oxidation within a 3-h timeframe. The pH value was recorded over a 2- to 4-min interval. After alkalinity dropped throughout the test, NaOH was added to maintain a pH of approximately 7.5 (within the range of 7.3–7.8) throughout the test.

Specific NH_4^+ oxidation rates (SAOR, mgN $gVSS^{-1}$ h^{-1}) and specific NO_2^- oxidation rates (SNOR, mgN $gVSS^{-1}$ h^{-1}) were used to estimate the oxidation of NH_4^+ and NO_2^- based on the following equations (Zhou et al., 2020):

$$\mathrm{SAOR}(\mathrm{mgNgVS^{-1}h^{-1}}) = \frac{(\mathrm{CNH_4 - N_{t1}}) - (\mathrm{CNH_4 - N_{t2}})}{\mathrm{VSS} \times (t_2 - t_1)},$$

$$\mathrm{SNOR}(\mathrm{mgNgVS^{-1}h^{-1}}) = \frac{(\mathrm{CNO_2 - N_{t1}}) - (\mathrm{CNO_2 - N_{t2}})}{\mathrm{VSS} \times (t_2 - t_1)},$$

where CNH_4-N_{t1} and CNO_2-N_{t1} are the concentration of NH_4^+-N and NO_2^--N and VSS was the volatile suspended solids.

FA and FNA were calculated using the following equations (Anthonisen et al., 1976):

$$\mathrm{FA}(\mathrm{mgL^{-1}}) = \frac{\left[\mathrm{NH_4^+ - N + NH_3 - N}\right] \times 10^{\mathrm{pH}}}{10^{\mathrm{pH}} + \exp\left(\frac{6{,}344}{273 + T}\right)},$$

where $\mathrm{NH_4^+ - N + NH_3 - N}$ is the total ammonia and T is the temperature tested during the batch tests.

$$\mathrm{FNA}(\mathrm{mgL^{-1}}) = \frac{[\mathrm{NO_2^- - N}]}{e^{\frac{-2{,}300}{T}} \times 10^{\mathrm{pH}}},$$

where $\mathrm{NO_2^- - N}$ is the concentration of NO_2^- and T is the temperature tested during the batch tests.

The NO_2^- accumulation ratio (NAR) was calculated with the following equation (Roots et al., 2020):

$$NAR(\%) = \frac{(\mathrm{CNO_2 - N_{t2}}) - (\mathrm{CNO_2 - N_{t1}})}{(\mathrm{CNO_2 - N_{t2}}) - (\mathrm{CNO_2 - N_{t1}}) + (\mathrm{CNO_3 - N_{t2}}) - (\mathrm{CNO_3 - N_{t1}})} \times 100,$$

where CNO_2-N_{t1} and CNO_3-N_{t1} were the concentration of NO_2^- and NO_3^- at different timepoints during the experiments.

DNA extraction and 16S amplicon sequencing

To shed light on key nitrogen-cycling taxa in both PAD reactors, biomass from each PAD reactor was investigated for DNA community analysis. Therefore, microbial community data reflect the full-scale PAD reactors from the single time point they were collected. The biomass of each sample was concentrated into a pellet by centrifuging a 2 ml aliquot at 13,000 RCF for 5 min and discarding the supernatant. DNA from each sample pellet was extracted using the Qiagen DNeasy PowerSoil Pro kit (Qiagen, Germany) on a QIAcube Connect (Qiagen, Germany) automated sample processor using manufacturer's SOP. DNA yield was quantified using Qubit HS dsDNA assay (Thermo Fisher Scientific, MA). rRNA Amplicon Generation PCR was performed on each DNA extract using primers Bakt_341F and Bakt_805R (Herlemann et al., **2011**) to target and amplify the V3-V4 hypervariable region of the 16S rRNA gene. Amplicon size was confirmed using gel electrophoresis. Illumina libraries were prepped from the generated amplicons and sequenced on a 2 × 300 Illumina MiSeq sequence run.

Sequencing data analysis

The raw sequences resulting from the MiSeq run was processed using the Quantitative Insights Into Microbial Ecology2 (QIIME2, v. 2021.4) (Bolyen et al., **2019**) pipeline. First, primer sequences and adapter sequences were trimmed from the raw reads and filtered for quality using the Qiime2 cutadapt plugin (Martin, **2011**). The Qiime2 dada2 plugin (Callahan et al., **2016**) was used to merge, denoise, and dereplicate the trimmed reads. The resulting reads were then used by dada2 to generate an amplicon sequence variant table (ASV) and a representative sequences file. Taxonomy for the data was assigned using the Qiime2 naïve Bayesian classifier (Pedregosa et al., **2011**) that was trained using the SILVA 138.1 database (Quast et al., **2013**; Yilmaz et al., **2014**). The representative sequences were aligned using the Qiime2 MAFFT plugin (Katoh & Standley, **2013**), and the alignment was masked using the Qiime2 mask plugin (Stackebrandt & Goodfellow, **1991**). The masked alignment was used as input for the Qiime2 phylogeny fasttree plugin (Price et al., **2010**) to generate a rooted phylogenetic tree.

The processed data were normalized and analyzed in R version 4.1.1 (R Core Team, **2021**). The ASV table was normalized to account for biases against sequencing depth and testing using the cumulative-sum scaling method (CSS) implemented in the R package metagenomeSeq (Paulson et al., **2013**). Analysis and visualization of the data in R was performed using packages, ampviz2 (Andersen et al., **2018**), dplyr (Wickham & François, **2014**), data.table (Dowle & Srinivasan, **2020**), ggplot2 (Wickham, **2011**), and phyloseq (McMurdie & Holmes, **2013**), together with the Midas field guide functional guild DB (Dueholm et al., **2022**; Nierychlo et al., **2020**).

RESULTS AND DISCUSSION

Lab-scale reactors demonstrate NO_2^- production and accumulation

Temperature impacts Ammonia removal and nitrite production rates

PAD test B and PAD test B were conducted in parallel reactors to determine how N removal mechanisms varied as a function of temperature. As shown in Figure **2a–c**, temperatures affected the nitrogen transformation rates in both reactors. For PAD test D seeded with biomass from the Denver MWR NTP, the NH_4^+ oxidation rates at 40°C and 50°C were similar, and they were both higher than the rates at 24.5°C and 30°C. The NH_4^+ oxidation rates of PAD test B showed a constant increase with increasing temperature through 40°C. Interestingly, the oxidation rate dropped to the lowest value at

50°C indicating this temperature was outside the operating range for the nitrifying community in the PAD's test B biomass (McNamara et al., **2022**) (Figure **2a**). This removal was likely due in part to air stripping as discussed later in Section **3.3**.

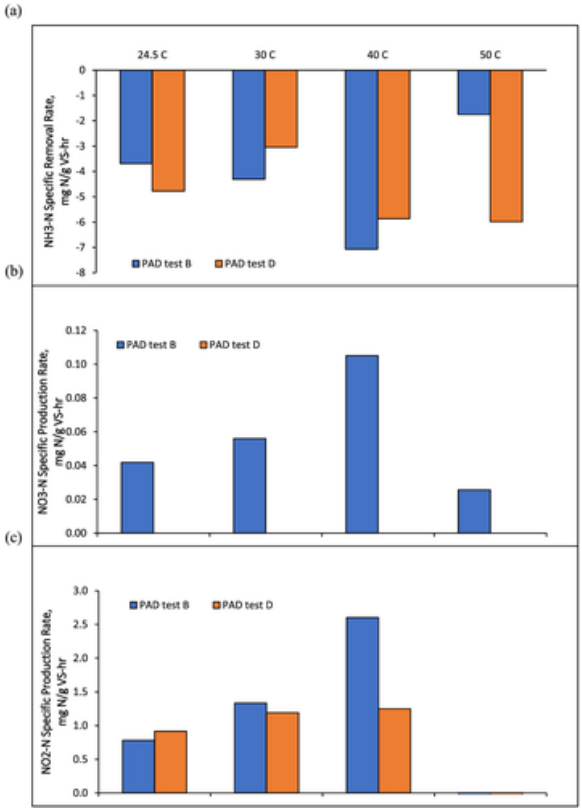

FIGURE 2 Comparison of nitrifying performance for PAD test B and PAD test D under different temperatures. (a) NH_4^+ removal and (b) NO_2^- and (c) NO_3^- production as a function of biomass source

Figure **2b** shows the comparison of NO_2^- accumulation. Both PAD test B and PAD test D showed high specific NO_2^- accumulation rates at 24.5°C, 30°C, and 40°C. Of note is the specific rate of NO_2^- accumulation in PAD test B at 40°C which is almost three times the one of PAD test D. Finally, neither tests had any NO_2^- accumulation at 50°C.

PAD test B had low levels of NO_2^- oxidation, suggesting that an active NOB community was not present (Figure **2c**). Specifically, NO_2^- oxidation rates were 0 to <1 mg N L^{-1}. The NO_2^- accumulation rates were 20–40% of the observed NH_4^+ oxidation rates (Figure **S1** and Table **S1**), while the rate of NO_3^- production was nearly zero (i.e., NO_3^- did not accumulate during the oxidation of NH_4^+; Figure **2c**). PAD test D also had low levels of NO_2^- oxidation, suggesting again that an active NOB community was not present or had limited activity. NO_2^- oxidation rates were 0 or <1 mgN L^{-1}. NO_2^- accumulation rates were 20–40% that of the observed ammonium oxidation rates (Figure **S2** and Table **S2**).

PAD test D 50°C NH_4^+-N high removal rate was not associated with NO_3^- or NO_2^- accumulation suggesting other potential mechanisms for NH_4^+ removal at elevated temperatures. This is in line with earlier studies where the nitrogen removal mechanism at higher temperatures has been linked to NH_4^+ stripping and biomass assimilation (Abeynayaka & Visvanathan, **2011**). This aspect will be further discussed in Section **3.3**. Finally, the difference in NH_4^+ oxidation rates can also be explained by the

different bacterial communities present in each biomass sample used (Section **3.2**). The full-scale PAD reactors operate with differences that may impact overall bacterial populations and therefore the NH_4^+ oxidation rates (Zhang et al., **2021**). Higher NH_4^+ oxidation rates from batch studies match full-scale data from Boulder where lower SRT operation showed higher NH_4^+ removal rates (McNamara et al., **2022**). Operating PAD reactors at low SRT values can still support good performance, for example, NH_4^+ removal, and a proper microbial community (McNamara et al., **2022**; Novak et al., **2011**).

In addition to specific oxidation rates, the nitrite accumulation ratio (NAR) for PAD test B (Figure **3a**) and PAD test D (Figure **3b**) were calculated at different temperatures as reported in the methods section. NAR has been used in earlier studies to explore mechanisms of nitrogen removal in bioreactors (Regmi et al., **2014**). The variability of temperatures did not appear to exert any impact on the NAR ratio indicating that NO_2^- accumulation was also sustained at higher temperatures (e.g., up to 40°C). The NAR ratio was calculated based on NO_2^- and NO_3^- concentrations (Table S3) during the tests performed at 24.5, 30 and 40°C while it was not calculated for 50°C batch test as no NO_2^- accumulation occurred (Figure **2b**). Interestingly, the NAR ratio was high at the initial timepoints for both PAD biomass samples (Figure **3a** and **3b**). This can be the result of a highly enriched biomass used as inoculum for both batch tests since both biomasses have a high propensity to accumulate NO_2^-. The NAR ratio tends to decrease at the end of the tests; this decrease is due to an overall lower availability of NH_4^+ (Figures **S1a** and **S2a**). Ratios higher than 100% are possibly due to fluctuations of NO_3^- (Figure **S1b** and S2b) that would overestimate NAR in the equation in the methods section (Section **2**). While dissolved oxygen was maintained at 4 mg L^{-1} and this would traditionally not provide an environment for NO_3^- reduction, high solids concentration and coarse bubble diffusion could provide anoxic pockets' that might have caused a loss of NO_3^- (McNamara et al., **2022**).

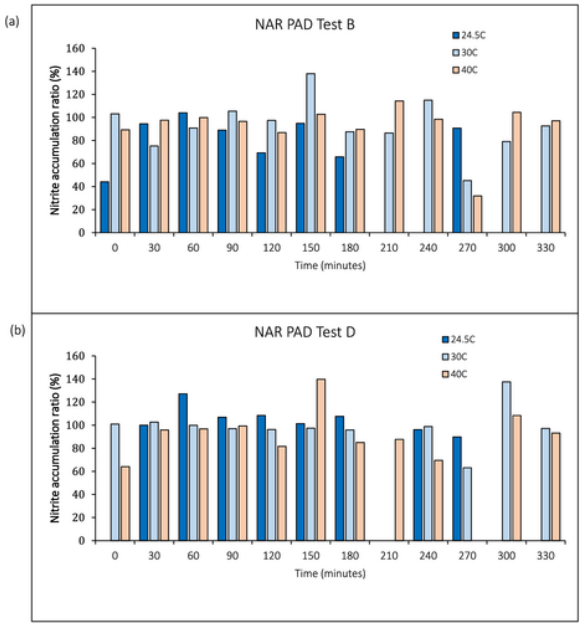

FIGURE 3 Nitrite accumulation ratio (NAR) in (a) PAD test B and (b) PAD test D batch study. NAR was not calculated for 50°C batch test as no NO_2^- accumulation occurred.

Impact of alkalinity and pH on nitrogen removal mechanisms

pH and alkalinity are significant controlling factors in nutrient removal systems, particularly those ones involving nitrification (Guisasola et al., **2007**). In our study, we carried out batch experiments to understand the impact of lime addition on N removal. Figure **4a,b** shows trends of pH, NO_2^- and TIC in batch experiments for PAD test B and PAD test D, respectively. PAD test B (Figure **4a**) shows a rather quick decrease in pH and TIC with subsequent NO_2^- accumulation. The pH decreases from approximately 8 to below 6.5 twice within the first 300 min of the experiment. NO_2^- accumulates to a final concentration of 105 mgN L^{-1}. PAD test D shows a rather slower decrease of pH (from 8 to 7.2) and TIC within the first 330 min of the experiment (Figure **4b**). NO_2^- accumulation does not go over the concentration of 70 mgN L^{-1}. The profiles and the behavior of both PAD test D and PAD test B confirm that the addition of alkalinity further stimulates nitrification (with NO_2^- accumulated as nitrification terminal product). While nitrification was augmented with alkalinity, NO_3^- did not accumulate despite O_2 being provided in excess. This reinforces the concept of this process occurring via NO_2^- shunt. This is well captured by the calculation of the overall specific rate of nitrite and nitrate production as shown in Figure **4c**. In all cases, the specific NO_2^- accumulation rate for all batch tests is higher than the NO_3^- accumulation (Figure **4c**) with a slightly higher production of NO_3^- from PAD's test B biomass.

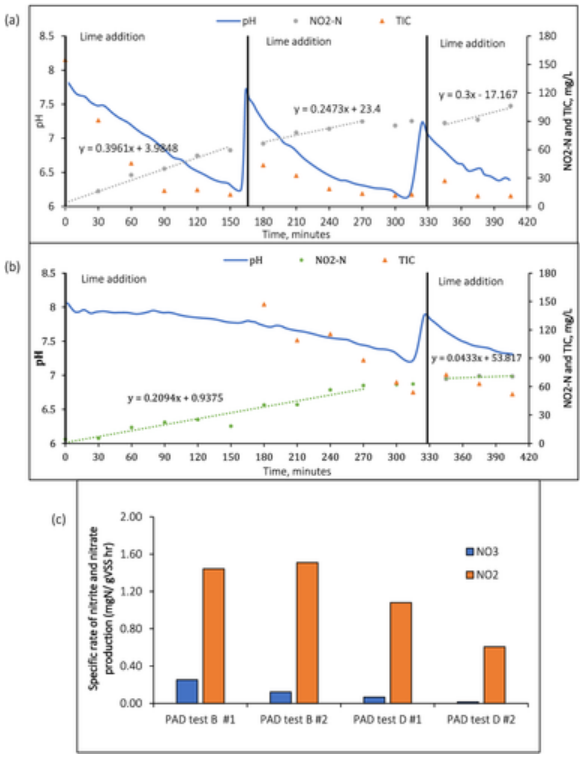

FIGURE 4 Batch profile trends of NO_2^- and TIC in the (a) PAD test B and (b) PAD test D. The respective batch tests are fitted with linear trend lines to estimate the observed in situ removal and accumulation rates. (c) Specific rates for NO_2^- and NO_3^- production in PAD test B and PAD test D

McNamara et al. (**2022**) showed that Boulder full-scale PAD reactor operates at pH values near neutral while Denver operates below neutral values. Excess lime addition during routine operation of the plant causes the biomass to be exposed to high pH levels (around 8.0) with decreased performance and potential accumulation of inhibitory compounds such as FA. The authors concluded that, for healthy

operations of PAD reactors, pH should be in the range 6.0–7.5 and that different ammonia removal rates between the plants might have been due to differences in microbial community compositions. To explore this hypothesis, we carried out a community composition analysis and confirmed differences for both biomasses (Section **3.2**).

Microbial community and diversity drive biological nitrogen removal during PAD

The microbial communities of the two different biomasses were characterized by IIIumina Miseq paired-end sequencing of 16S rRNA gene (Figures **5** and **6**). Observed and Shannon-Wiener diversity were estimated for both samples (Figure **5a,b**). The observed diversity is a measure of diversity of a sample that considers the species' richness. The Shannon-Wiener diversity index instead is a metric for entropy and species diversity that takes into account the species' relative abundance (Fan et al., **2022**). PAD's test B biomass showed a higher observed richness (Figure **5a**) and Shannon-Wiener diversity (Figure **5b**) than PAD's test D biomass. Despite both reactors performing the same function, their communities were different based on diversity. In general, diverse communities are expected to handle perturbations better than communities with lower diversity (Awasthi et al., **2014**; Shade et al., **2012**). Indeed, Denver's full-scale plant underwent more process fluctuations following perturbations (McNamara et al., **2022**).

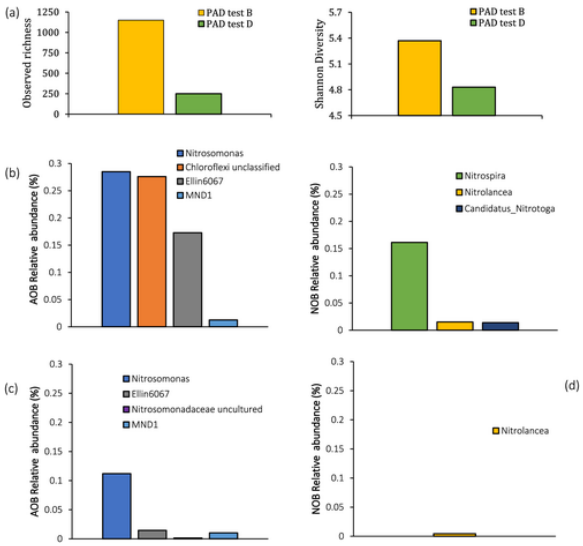

FIGURE 5 (a) Observed richness and (b) Shannon Diversity Assessment for the PAD's test B and D biomasses. Comparison of AOB and NOB relative abundance for biomass from (c) PAD test B and (d) PAD test D, respectively

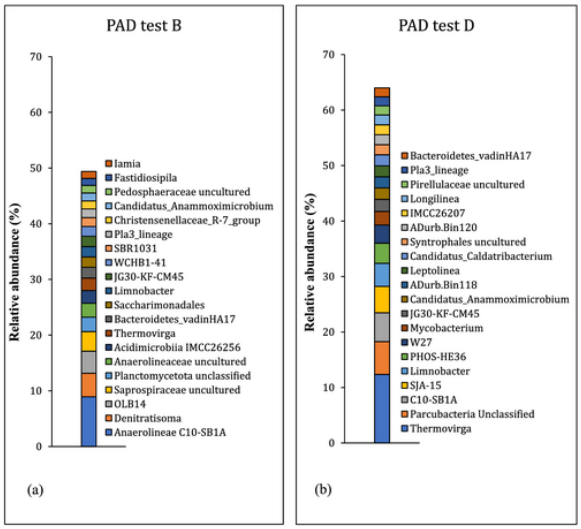

FIGURE 6 Top 20 genera in (a) PAD's test B and (b) PAD's test D biomass

The microbial community structure at the genus level was further analyzed to reveal key players of the nitrogen cycle in the PAD reactors. A comparison of the nitrifier abundances (AOB and NOB) is shown in Figure **5c,d**. The comparison of AOB relative abundances between the PAD's test D and PAD's test B biomass indicates over two times higher relative abundance for the PAD test B biomass (Figure **5c**). This higher relative abundance can be driven by a lower SRT (McNamara et al., **2022**), requiring increased AOB populations for an equivalent specific rate, whereas Denver's full-scale SRT is approximately three times that of the Boulder full-scale PAD reactor which can decrease overall abundance. NOB relative abundances confirm observations of the in situ NO_3^- specific rates between the reactors. The PAD's test D biomass NOB relative abundance is near zero, while the PAD's test B biomass indicates presence of a low NOB population (Figure **5d**). One of the observed differences that indicate a difference in the AOB and NOB populations between PAD's test D and B biomass is the NO_3^- specific rate (Figure **2c**). While both NO_3^- specific rates were low, PAD's test D biomass indicated a rate of zero or near zero suggesting a significant out selection or suppression of NOB activity.

Different factors can be responsible for shaping the composition of the full-scale PAD reactors in Denver and Boulder. These include temperature, ordinary heterotrophic organisms (OHOs) competition for NO_2^-, SRT, and NH_4^+ loadings. Temperature is a key parameter for nitrification greatly affecting the rates of nitrifying bacteria (McNamara et al., **2022**). Previous studies have shown that optimal temperature for nitrification occur at 28–36°C (Guo et al., **2010**) while it is believed that high temperature operation (e.g., 35°C) can be a successful strategy to achieve nitritation (Hellinga et al., **1998**). Additionally, the outcompetition of NOB can be explained by a higher sensitivity of NOB to higher temperatures than AOB as outlined by González-Martínez et al. (**2011**). OHOs can also play an important role in the outcompetition of NOB. OHOs thrive in a carbon-rich and low DO environment as suggested from full-scale operation of PAD reactors in McNamara et al. (**2022**). Their fast growth rate and ideal growth conditions lead to outcompete NOB successfully over NO_2^- (Winkler et al., **2012**).

The higher diversity observed in PAD's test B biomass due to different SRT operation could be another key player for Boulder's higher resilience to perturbations as shown in McNamara et al. (**2022**). Sui et al. (**2020**) evaluated different strategies including a short SRT, to improve nitritation, and were able to

achieve a high NAR ratio (81%) along with a selection of AOB at the expense of the NOB that were washed out. The selection of microbial communities to enhance NH_4^+ removal has been also reported in other studies (Neissi et al., **2022**). Higher NH_4^+ performance of Boulder PAD's biomass at full-scale (McNamara et al., **2022**) and in our study can be correlated with higher AOB relative abundance (Figure **5c**) and a higher species' richness in PAD's test B biomass (Figure **5a**). The higher abundance of AOB under these conditions suggests a potential competitive advantage. Another hypothesis is that the full-scale PAD in Boulder receives higher NH_4^+ loadings (McNamara et al., **2022**), and this could explain the higher bacterial diversity along with a higher AOB abundance. Ye and Zhang (**2011**) showed that AOB can become the dominant players and have a 40 times higher abundance than other microorganisms in nitrifying reactors under high NH_4^+ loadings.

The composition of AOB is quite similar with *Nitrosomonas* being the key genera in both samples (Figure **5c,d**). Other shared bacteria include the uncultured genus *Ellin6067* and MND1, belonging to the family Nitrosomonadaceae are also of note and are both involved in NH_4^+ oxidation processes (Wang et al., **2021**; Yu et al., **2021**). *Chloroflexi* here identified at the phylum level was only found in the PAD's test B biomass sample (Figure **5c**); this phylum has been often found associated with thermophilic environment and with NH_4^+ oxidation (Herber et al., **2020**). NOB was found to have the lowest or negligible abundance in both samples except for *Nitrospira* in PAD's test B sample. The genus *Nitrospira* has been proposed as a key and predominant NOB especially under low dissolved oxygen (Mehrani et al., **2020**) and has been observed for the first time in a full-scale wastewater treatment operating at 50°C (Lopez-Vazquez et al., **2014**). The presence of *Nitrospira* could explain some of the NO_2^- consumption and the subsequent NO_3^- formation (Figure **S2b**). However, the formation of NO_3^- is impact by high temperatures, for example, 50°C. As mentioned earlier, different studies have reported the inhibition of NOB by high temperatures (Guo et al., **2010**; Hellinga et al., **1998**). Besides temperature, other parameters including FA can potentially influence the abundance and activity of NOB; this will be further discussed in Section **3.3**. Overall, all these parameters synergistically contribute to the NOB outcompetition.

Figure **6** shows the top 20 genera for both PAD's test B and D biomass samples (Figure **6a,b**, respectively). As mentioned earlier, the two samples differ for their diversity. This can also be observed in Figure **6a,b** where a lower diversity can be observed for the PAD's test D sample with the top 20 genera representing roughly 65% of the final bacterial community. The PAD's test D biomass is dominated by fermenting bacteria (Figure **6b**) with *Thermovirga* being the most abundant genus at over 10% abundance; *Thermovirga* has been mainly found in anaerobic digesters (Li et al., **2016**). This is in line with our findings as the biomasses used for this study and feeding both Boulder's and Denver's PAD reactors receive effluent from mesophilic anaerobic digesters (McNamara et al., **2022**). *Thermovirga* is also present in PAD's test B biomass but at a lower relative abundance (Figure **6a**). Overall, PAD test D has almost 20% of the overall biomass characterized by fermenting bacteria (Figure **6b**). This is three times the fermenting bacteria population of the PAD's test B biomass (Figure **6a**) and is likely a result of the long SRT in the Denver full-scale reactor. Longer SRTs are usually linked with a selection for slow growing microbes that process substrate slowly and with an enhanced hydrolysis of slowly biodegradable substrates, actuated by fermenting bacteria (Grady et al., **2011**; McNamara et al., **2022**). Finally, the community of each biomass is composed of a high abundance of

denitrifying bacteria with some examples including *Limnobacter* in PAD's test D biomass and *Denitratisoma* (Qiao et al., **2022**) in PAD's test B biomass (Figure **6a,b**).

Temperature, pH, and nitrogen speciation could lead to different nitrogen loss routes

The batch tests from Section **3.1** and the community analysis from Section **3.2** showed interesting trends and specific mechanisms of nitrogen removal. However, some TIN mass balances (Figure **S3**) show a decreasing trend over time. This suggests that other mechanisms of nitrogen loss are taking place. For example, the PAD test D 50°C NH_4^+ high removal rate is not associated with NO_2^- or NO_3^- accumulation suggesting NH_4^+ removal at 50°C possibly linked to ammonia off gassing. Figure **7** provides a comparison of the ammonia gas present at a range of pH and temperatures. At a pH of 7.5 and pH of 8.0 and 50°C, approximately 9% and 30%, respectively, of the NH_4^+ is present as ammonia gas (Figure **7**). This is in line with what earlier studies have described. Courtens et al. (**2016**) performed hydraulic abiotic studies in test reactors and found that as high as 6 mgFA L^{-1} day^{-1} was stripped at pH 8, 50°C and 20 mg NH_4^+ L^{-1}. In our study, higher aeration rates of the reactors (saturated DO around 4 mg L^{-1}) could lead to elevated stripping rates. This effect would also lead to predicted higher NH_4^+ specific removal rates.

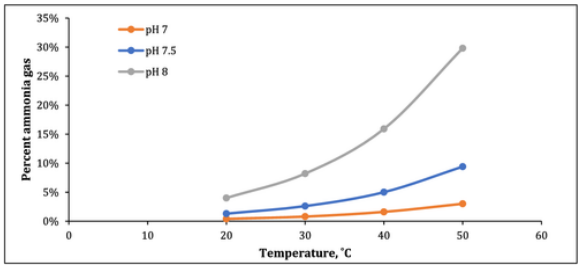

FIGURE 7 Ammonia nitrogen percent of ammonia gas present at pH 7, 7.5, and 8 for the temperature range 20–50°C

Another route for nitrogen loss is the production of N_2O. N_2O is a potent greenhouse gas and can be produced during nitrification and denitrification (Sabba et al., **2017**). PAD reactors experience both a high NH_4^+ loading and high production of NO_2^- (McNamara et al., **2022**). Both parameters (as well as possible swings in DO) can lead to high N_2O emissions during nitrification via the nitrifier denitrification pathway (Sabba et al., **2015**). A recent study confirmed that NO_2^- variation can explain poorer correlation between N_2O and total nitrogen removal. The authors also concluded that N_2O emissions are a crucial parameter to track during nitritation-denitritation processes (Kuokkanen et al., **2021**). Shifts in DO, coarse bubble diffusion, and solids' concentration can provide additional mechanisms for nitrogen loss that include partial heterotrophic denitrification and traditional denitritation/denitritation. Partial heterotrophic denitrification can be the result of selective inhibition of the nitrous oxide reductase enzyme, due to DO, that prevents N_2O from being further reduced to nitrogen gas (Guo et al., **2018**; Sabba et al., **2017**). Traditional denitritation/denitritation with removal of NO_2^- and/or NO_3^- and heterotrophic production of nitrogen gas can also affect TIN mass balance (Daigger, **2014**). As mentioned earlier in Section **3.1.1**, this is possible when high solids concentration and coarse bubble diffusion create a favorable environment for the formation of anoxic pockets where production of nitrogen gas occurs (McNamara et al., **2022**). Finally, the TIN mass balance (Figure **S3**) could also be impacted by biological uptake of nitrogen through bacterial growth and likely accounts

for a small portion (<5%) (Courtens et al., **2014**). In our study, we focused on the fate of nitrogen at constant saturated DO, while future work should look at TN and other nitrogen species, such as N_2O.

As seen in Section **3.1** and in McNamara et al. (**2022**), the operation of full-scale PAD reactors involves high loadings of NH_4^+ along with high production of NO_2^-. For this reason, some additional important considerations involve the potential formation/presence of FA that, besides being a substrate for AOB, can also have potential inhibitory effects at high concentrations. The FA concentration can vary with pH, temperature, and ammonium concentration (Anthonisen et al., **1976**). Based on literature, the ranges of inhibition can vary between 10–150 and 18–51 mg L^{-1}, for AOB and NOB, respectively (Anthonisen et al., **1976**; Vadivelu et al., **2007**; Zhang et al., **2018**). It is of note that NOB are inhibited by lower concentrations of FA than AOB (Zhang et al., **2018**). In our study to match the full-scale nitrogen loadings, experiments were ran in batch mode with NH_4^+ in the range of concentration of 800–1,100 mgN L^{-1} for both biomasses at a pH of 7.5 and temperatures of 24.5°C, 30°C, 40°C, and 50°C (Figure **S1a** and S2a) with a potential FA concentration range of 15–45 mgFA L^{-1}. Some of the high FA values could explain the lower rate of nitrate production (Figure **2c**) and low abundance of NOB (Figure **5c** and **5d**). However, our study used enriched biomass from full-scale PAD reactors, with an existing and established community of AOB. We used elevated DO to drive for higher NO_3^- production that did not occur and confirmed the relevance of the AOB population in these reactors. This is in line with full-scale PAD reactors where NO_2^- accumulation was observed (McNamara et al., **2022**). Furthermore, differently from our batch experiments, the operation of the full-scale PAD reactors does not experience the same final concentration of NH_4^+ since they are operated as continuous stirred-tank reactors (CSTRs). Similarly, some of the NO_3^- observed in our batch study and in the full-scale PAD reactors could be attributed to a partial inhibition of the NOB. Gu et al. (**2007**) investigated the nitrifying community structure in a single-stage submerged attached-growth bioreactor for treatment of high-strength NH_4^+ wastewater and found that high FA concentration could inhibit NO_2^- oxidation but would unlikely washout the NOB from the system. Similarly, Courtens et al. (**2016**) enriched autotrophic thermophilic nitrifiers and transferred them to a bioreactor operating at 50°C. Interestingly, the community was composed of 17% AOA and 25% NOB, and FA had 33% more detrimental effects on NOB's specific activities. The range of inhibition levels can depend on acclimatization of the biomass at high concentrations, temperature, and solids (nitrifiers) concentration (Gu et al., **2007**).

CONCLUSIONS

Research previously reported operation and performance of reactors, but no information was provided on key mechanisms for nitrogen removal. Here, we carried out tests at different temperatures with two different biomasses from full-scale PAD reactors and found that nitritation is the dominant route to remove nitrogen. Our results show that NO_2^- accumulated at concentrations as high as 150 mg N L^{-1}. Neither PAD batch test indicated NH_4^+ oxidation to NO_2^- at 50°C, although removal was observed. This suggests alternative mechanisms for nitrogen loss, including ammonia stripping. Moreover, alkalinity was found important for sustaining optimal nitrogen removal and can be added to overcome onsite alkalinity limitations. Finally, both PAD samples' bacterial community showed a higher relative abundance of AOB and a rather low or not existing presence of NOB confirming NO_2^- shunt as the predominant mechanism of nitrogen removal in these systems.

ACKNOWLEDGMENTS

The authors would like to thank Christopher Marks at the Boulder Wastewater Treatment Facility (Boulder) and Dr. Thomas Worley-Morse at Metro Water Recovery (Denver) for providing the samples and for the in-depth discussions of operational facilities. Additionally, we would like to thank Ameer Hyder and operations with the Trinity River Authority for onsite testing facilities and assistance.

DATA AVAILABILITY STATEMENT

The data that supports the findings of this study are available in the supplementary material of this article.

Supporting Information

Filename	Description
wer10762-sup-0001-Suppinfo_latest.docxWord 2007 document , 12.5 MB	**Table S1:** PAD test D observed and specific nitrification rates at different temperatures **Table S2:** PAD test B observed and specific nitrification rates at different temperatures **Table S3:** Concentration of nitrite and nitrate in (a-b) PAD test B and (c-d) PAD test D at different temperatures **Figure S1:** PAD test D nitrification rates at 24.5, 30, 40, and 50°C. **Figure S2:** PAD test B nitrification rates at 24.5, 30, 40, and 50°C. **Figure S3:** Total inorganic nitrogen balance for (a) PAD test D and (b) PAD test B biomass **Figure S4:** Calculated free ammonia estimation for PAD test B (line) and Pad test D (line with squares) biomass over time **Figure S5:** Calculated free nitrous acid for PAD test B (line) and Pad test D (line with squares) biomass over time

Please note: The publisher is not responsible for the content or functionality of any supporting information supplied by the authors. Any queries (other than missing content) should be directed to the corresponding author for the article.

REFERENCES

Abeynayaka, A., & Visvanathan, C. (2011). Mesophilic and thermophilic aerobic batch biodegradation, utilization of carbon and nitrogen sources in high-strength wastewater. *Bioresource Technology*, **102**(3), 2358– 2366. https://doi.org/10.1016/j.biortech.2010.10.096

Ahmad, M., Denee, M. A., Jiang, H., Eskicioglu, C., Kadota, P., & Gregonia, T. (2016). Sequential anaerobic/aerobic digestion for enhanced carbon/nitrogen removal and cake odor reduction. *Water Environment Research*, **88**(12), 2233– 2244. https://doi.org/10.2175/106143016X14504669768291

Andersen, K. S., Kirkegaard, R. H., Karst, S. M., & Albertsen, M. (2018). ampvis2: An R package to analyse and visualise 16S rRNA amplicon data. *BioRxiv*, 299537.

Anthonisen, A. C., Loehr, R. C., Prakasam, T. B., & Srinath, E. G. (1976). Inhibition of nitrification by ammonia and nitrous acid. *Journal - Water Pollution Control Federation*, **48**, 835– 852.

Awasthi, A., Singh, M., Soni, S. K., Singh, R., & Kalra, A. (2014). Biodiversity acts as insurance of productivity of bacterial communities under abiotic perturbations. *The ISME Journal*, **8**(12), 2445– 2452. https://doi.org/10.1038/ismej.2014.91

Bauer, H., Johnson, T. D., Johnson, B. R., Oerke, D., & Graziano, S. (2016). Comparison of sidestream treatment technologies: Post aerobic digestion and anammox. *Water Science and Technology*, **73**(11), 2789– 2803. https://doi.org/10.2166/wst.2016.079

Bolyen, E., Rideout, J. R., Dillon, M. R., Bokulich, N. A., Abnet, C. C., Al-Ghalith, G. A., Alexander, H., Alm, E. J., Arumugam, M., Asnicar, F., Bai, Y., Bisanz, J. E., Bittinger, K., Brejnrod, A., Brislawn, C. J., Brown, C. T., Callahan, B. J., Caraballo-Rodriguez, A. M., Chase, J., … Caporaso, J. G. (2019). Reproducible, interactive, scalable and extensible microbiome data science using QIIME 2. *Nature Biotechnology*, **37**, 852– 857.

Callahan, B. J., McMurdie, P. J., Rosen, M. J., Han, A. W., Johnson, A. J. A., & Holmes, S. P. (2016). DADA2: High-resolution sample inference from Illumina amplicon data. *Nature Methods*, **13**(7), 581– 583. https://doi.org/10.1038/nmeth.3869

Carey, D. E., McNamara, P. J., & Zitomer, D. H. (2015). Biochar from pyrolysis of biosolids for nutrient adsorption and Turfgrass cultivation. *Water Environment Research*, **87**(12), 2098– 2106. https://doi.org/10.2175/106143015X14362865227391

Carey, D. E., Yang, Y., McNamara, P. J., & Mayer, B. K. (2016). Recovery of agricultural nutrients from biorefineries. *Bioresource Technology*, **215**, 186– 198. https://doi.org/10.1016/j.biortech.2016.02.093

Chen, Q., Ni, J., Ma, T., Liu, T., & Zheng, M. (2015). Bioaugmentation treatment of municipal wastewater with heterotrophic-aerobic nitrogen removal bacteria in a pilot-scale SBR. *Bioresource Technology*, **183**, 25– 32. https://doi.org/10.1016/j.biortech.2015.02.022

Courtens, E. N., Boon, N., De Schryver, P., & Vlaeminck, S. E. (2014). Increased salinity improves the thermotolerance of mesophilic nitrification. *Applied Microbiology and Biotechnology*, **98**(10), 4691– 4699.

Courtens, E. N. P., Spieck, E., Vilchez-Vargas, R., Bodé, S., Boeckx, P., Schouten, S., Jauregui, R., Pieper, D. H., Vlaeminck, S. E., & Boon, N. (2016). A robust nitrifying community in a bioreactor at 50°C opens up the path for thermophilic nitrogen removal. *The ISME Journal*, **10**(9), 2293– 2303. https://doi.org/10.1038/ismej.2016.8

Daigger, G. T. (2014). Oxygen and carbon requirements for biological nitrogen removal processes accomplishing nitrification, nitritation, and anammox. *Water Environment Research*, **86**(3), 204– 209. https://doi.org/10.2175/106143013X13807328849459

Delgado Vela, J., Stadler, L. B., Martin, K. J., Raskin, L., Bott, C. B., & Love, N. G. (2015). Prospects for biological nitrogen removal from anaerobic effluents during mainstream wastewater treatment. *Environmental Science & Technology Letters*, **2**(9), 234– 244. https://doi.org/10.1021/acs.estlett.5b00191

Dowle, M., Srinivasan, A. (2020) data.table: Extension of 'data. frame'. 2019. R package version 1.12.8.

Dueholm, M. K. D., Nierychlo, M., Skytte Andersen, K. S., Rudkjøbing, V., Knutsson, S., Albertsen, M., & Nielsen, P. H. (2022). MiDAS 4: A global catalogue of full-length 16S rRNA gene sequences and taxonomy for studies of bacterial communities in wastewater treatment plants. *Nature Communications*, **13**(1), 1– 15.

Fan, Y., Zhang, M., Cheng, J., Yong, D., Ji, J., Wu, Q., & He, C. (2022). Elucidating nitrifying performance, nitrite accumulation and microbial community in a three-stage plug flow moving bed biofilm reactor (PF - MBBR). *Chemosphere*, **297**, 134087. https://doi.org/10.1016/j.chemosphere.2022.134087

González-Martínez, A., Poyatos, J. M., Hontoria, E., Gonzalez-Lopez, J., & Osorio, F. (2011). Treatment of effluents polluted by nitrogen with new biological technologies based on autotrophic nitrification-denitrification processes. *Recent Patents on Biotechnology*, **5**, 74– 84. https://doi.org/10.2174/187220811796365671

Grady, C. P. L., Daigger, G. T., Love, N. G., & Filipe, C. D. M. (2011). *Biological wastewater treatment*. CRC Press. https://doi.org/10.1201/b13775

Gu, A. Z., Pedros, P. B., Kristiansen, A., Onnis-Hayden, A., & Schramm, A. (2007). Nitrifying community analysis in a single submerged attached-growth bioreactor for treatment of high-ammonia waste stream. *Water Environment Research*, **79**(13), 2510– 2518. https://doi.org/10.2175/106143007X254566

Guisasola, A., Petzet, S., Baeza, J. A., Carrera, J., & Lafuente, J. (2007). Inorganic carbon limitations on nitrification: Experimental assessment and modelling. *Water Research*, **41**, 277– 286. https://doi.org/10.1016/j.watres.2006.10.030

Guo, J., Peng, Y., Huang, H., Wang, S., Ge, S., Zhang, J., & Wang, Z. (2010). Short- and long-term effects of temperature on partial nitrification in a sequencing batch reactor treating domestic wastewater. *Journal of Hazardous Materials*, **179**(1–3), 471– 479. https://doi.org/10.1016/j.jhazmat.2010.03.027

Guo, G., Wang, Y., Hao, T., Wu, D., & Chen, G. H. (2018). Enzymatic nitrous oxide emissions from wastewater treatment. *Frontiers of Environmental Science & Engineering*, **12**(1), 1– 12.

Hellinga, C., Schellen, A. A. J. C., Mulder, J. W., van Loosdrecht, M. C. M., & Heijnen, J. J. (1998). The sharon process: An innovative method for nitrogen removal from ammonium-rich waste water. *Water Science and Technology*, **37**(9), 135– 142. https://doi.org/10.2166/wst.1998.0350

Herber, J., Klotz, F., Frommeyer, B., Weis, S., Straile, D., Kolar, A., Sikorski, J., Egert, M., Dannenmann, M., & Pester, M. (2020). A single Thaumarchaeon drives nitrification in deep oligotrophic Lake Constance. *Environmental Microbiology*, **22**(1), 212– 228. https://doi.org/10.1111/1462-2920.14840

Herlemann, D. P. R., Labrenz, M., Jürgens, K., Bertilsson, S., Waniek, J. J., & Andersson, A. F. (2011). Transitions in bacterial communities along the 2000 km salinity gradient of the Baltic Sea. *The ISME Journal*, **5**(10), 1571– 1579. https://doi.org/10.1038/ismej.2011.41

Iannacone, F., di Capua, F., Granata, F., Gargano, R., & Esposito, G. (2020). Simultaneous nitrification, denitrification and phosphorus removal in a continuous-flow moving bed biofilm reactor alternating microaerobic and aerobic conditions. *Bioresource Technology*, **310**, 123453. https://doi.org/10.1016/j.biortech.2020.123453

Katoh, K., & Standley, D. M. (2013). MAFFT multiple sequence alignment software version 7: Improvements in performance and usability. *Molecular Biology and Evolution*, **30**(4), 772– 780. https://doi.org/10.1093/molbev/mst010

van Kessel, M. A., Speth, D. R., Albertsen, M., Nielsen, P. H., Opden Camp, H. J., Kartal, B., Jetten, M. S., & Lücker, S. (2015). Complete nitrification by a single microorganism. *Nature*, **528**(7583), 555– 559. https://doi.org/10.1038/nature16459

Kim, J., & Novak, J. T. (2011). Combined anaerobic/aerobic digestion: Effect of aerobic retention time on nitrogen and solids removal. *Water Environment Research*, **83**(9), 802– 806. https://doi.org/10.2175/106143011X12928814444970

Kuenen, J. G. (2008). Anammox bacteria: From discovery to application. *Nature Reviews Microbiology*, **6**(4), 320– 326. https://doi.org/10.1038/nrmicro1857

Kumar, N., Novak, J., & Murthy, S. (2006). Effect of secondary aerobic digestion on properties of anaerobic digested biosolids. *Proceedings of the Water Environment Federation*, **2006**(5), 6806– 6829. https://doi.org/10.2175/193864706783761527

Kuokkanen, A., Blomberg, K., Mikola, A., & Heinonen, M. (2021). Unwanted mainstream nitritation–denitritation causing massive N2O emissions in a continuous activated sludge process. *Water Science and Technology*, **83**(9), 2207– 2217. https://doi.org/10.2166/wst.2021.127

Li, L., He, Q., Ma, Y., Wang, X., & Peng, X. (2016). A mesophilic anaerobic digester for treating food waste: Process stability and microbial community analysis using pyrosequencing. *Microbial Cell Factories*, **15**, 65. https://doi.org/10.1186/s12934-016-0466-y

Liu, Z., Mayer, B. V., Seyedi, S., Raju, K. K., Arun, S. K. Z., McNamara, D., & Patrick, J. (2020). The State of Technologies and Research for Energy Recovery from Municipal Wastewater Sludge and Biosolids. *Current Opinion in Environmental Science & Health*, **14**, 31– 36. https://doi.org/10.1016/j.coesh.2019.12.004

Lopez-Vazquez, C. M., Kubare, M., Saroj, D. P., Chikamba, C., Schwarz, J., Daims, H., & Brdjanovic, D. (2014). Thermophilic biological nitrogen removal in industrial wastewater treatment. *Applied Microbiology and Biotechnology*, **98**, 945– 956. https://doi.org/10.1007/s00253-013-4950-6

Mannina, G., Badalucco, L., Barbara, L., Cosenza, A., di Trapani, D., Gallo, G., Laudicina, V. A., Marino, G., Muscarella, S. M., Presti, D., & Helness, H. (2021). Enhancing a transition to a circular economy in the water sector: The EU project WIDER UPTAKE. *Water*, **13**(7), 946. https://doi.org/10.3390/w13070946

Martin, M. (2011). Cutadapt removes adapter sequences from high-throughput sequencing reads. *EMBnet. Journal*, **17**(1), 10– 12. https://doi.org/10.14806/ej.17.1.200

McMurdie, P. J., & Holmes, S. (2013). Phyloseq: An R package for reproducible interactive analysis and graphics of microbiome census data. *PLoS ONE*, **8**(4), e61217. https://doi.org/10.1371/journal.pone.0061217

McNamara, P., Sabba, F., Redmond, E., Dunlap, P., Worley-Morse, T., Marks, C., & Downing, L. (2022). Post aerobic digestion (PAD) is a solids Sidestream nutrient removal process that utilizes native carbon: Performance and key operational parameters from two full-scale PAD reactors. *Environmental Science; Advances*, **1**, 216– 228. https://doi.org/10.1039/D2VA00045H

Mehrani, M.-J., Sobotka, D., Kowal, P., Ciesielski, S., & Makinia, J. (2020). The occurrence and role of Nitrospira in nitrogen removal systems. *Bioresource Technology*, **303**, 122936. https://doi.org/10.1016/j.biortech.2020.122936

Neissi, A., Rafiee, G., Rahimi, S., Farahmand, H., Pandit, S., & Mijakovic, I. (2022). Enriched microbial communities for ammonium and nitrite removal from recirculating aquaculture systems. *Chemosphere*, **295**, 133811. https://doi.org/10.1016/j.chemosphere.2022.133811

Nierychlo, M., Andersen, K. S., Xu, Y., Green, N., Jiang, C., Albertsen, M., Dueholm, M. S., & Nielsen, P. H. (2020). MiDAS 3: An ecosystem-specific reference database, taxonomy and knowledge platform for activated sludge and anaerobic digesters reveals species-level microbiome composition of activated sludge. *Water Research*, **182**, 115955. https://doi.org/10.1016/j.watres.2020.115955

Novak, J. T., Banjade, S., & Murthy, S. N. (2011). Combined anaerobic and aerobic digestion for increased solids reduction and nitrogen removal. *Water Research*, **45**, 618– 624. https://doi.org/10.1016/j.watres.2010.08.014

Parravicini, V., Svardal, K., Hornek, R., & Kroiss, H. (2008). Aeration of anaerobically digested sewage sludge for COD and nitrogen removal: Optimization at large-scale. *Water Science and Technology*, **57**, 257– 264. https://doi.org/10.2166/wst.2008.020

Paulson, J. N., Stine, O. C., Bravo, H. C., & Pop, M. (2013). Differential abundance analysis for microbial marker-gene surveys. *Nature Methods*, **10**, 1200– 1202. https://doi.org/10.1038/nmeth.2658

Pedregosa, F., Varoquaux, G., Gramfort, A., Michel, V., Thirion, B., Grisel, O., Blondel, M., Prettenhofer, P., Weiss, R., Dubourg, V., Vanderplas, J., Passos, A., Cournapeau, D., Brucher, M., Perrot, M., & Duchesnay, É. (2011). Scikit-learn: Machine learning in Python. *Journal of Machine Learning Research*, **12**, 2825– 2830.

Price, M. N., Dehal, P. S., & Arkin, A. P. (2010). FastTree 2--approximately maximum-likelihood trees for large alignments. *PLoS ONE*, **5**(3), e9490. https://doi.org/10.1371/journal.pone.0009490

Qiao, L., Yuan, Y., Mei, C., Yin, W., Zou, C., Yin, Y., Guo, Q., Chen, T., & Ding, C. (2022). Reinforced nitrite supplement by cathode nitrate reduction with a bio-electrochemical system coupled anammox reactor. *Environmental Research*, **204**, 112051. https://doi.org/10.1016/j.envres.2021.112051

Quast, C., Pruesse, E., Yilmaz, P., Gerken, J., Schweer, T., Yarza, P., Peplies, J., & Glöckner, F. O. (2013). The SILVA ribosomal RNA gene database project: Improved data processing and web-based tools. *Nucleic Acids Research*, **41**, D590– D596. https://doi.org/10.1093/nar/gks1219

R Core Team. (2021). R: A Language and Environment for Statistical Computing, **2015**.

Rahimi, S., Modin, O., & Mijakovic, I. (2020). Technologies for biological removal and recovery of nitrogen from wastewater. *Biotechnology Advances*, **43**, 107570. https://doi.org/10.1016/j.biotechadv.2020.107570

Regmi, P., Miller, M. W., Holgate, B., Bunce, R., Park, H., Chandran, K., Wett, B., Murthy, S., & Bott, C. B. (2014). Control of aeration, aerobic SRT and COD input for mainstream nitritation/denitritation. *Water Research*, **57**, 162– 171. https://doi.org/10.1016/j.watres.2014.03.035

Roots, P., Sabba, F., Rosenthal, A. F., Wang, Y. B., Yuan, Q., Rieger, L., Yang, F. H., Kozak, J. A., Zhang, H., & Wells, G. F. (2020). Integrated shortcut nitrogen and biological phosphorus removal from mainstream wastewater: Process operation and modeling. *Environmental Science: Water Research.*, **6**(3), 566– 580. https://doi.org/10.1039/C9EW00550A

Roots, P., Wang, Y., Rosenthal, A. F., Griffin, J. S., Sabba, F., Petrovich, M., Yang, F., Kozak, J. A., Zhang, H., & Wells, G. F. (2019). Comammox Nitrospira are the dominant ammonia oxidizers in a mainstream low dissolved oxygen nitrification reactor. *Water Research*, **157**, 396– 405. https://doi.org/10.1016/j.watres.2019.03.060

Sabba, F., Picioreanu, C., Boltz, J. P., & Nerenberg, R. (2017). Predicting N2O emissions from nitrifying and denitrifying biofilms: A modeling study. *Water Science and Technology*, **75**(3), 530– 538. https://doi.org/10.2166/wst.2016.484

Sabba, F., Picioreanu, C., & Nerenberg, R. (2017). Mechanisms of nitrous oxide (N2 O) formation and reduction in denitrifying biofilms. *Biotechnology and Bioengineering*, **114**(12), 2753– 2761. https://doi.org/10.1002/bit.26399

Sabba, F., Picioreanu, C., Perez, J., & Nerenberg, R. (2015). Hydroxylamine diffusion can enhance N(2)O emissions in nitrifying biofilms: A modeling study. *Environmental Science & Technology*, **49**(3), 1486– 1494. https://doi.org/10.1021/es5046919

Sabba, F., Terada, A., Wells, G., Smets, B. F., & Nerenberg, R. (2018). Nitrous oxide emissions from biofilm processes for wastewater treatment. *Applied Microbiology and Biotechnology*, **102**(22), 9815– 9829. https://doi.org/10.1007/s00253-018-9332-7

Shade, A., Peter, H., Allison, S. D., Baho, D. L., Berga, M., Bürgmann, H., Huber, D. H., Langenheder, S., Lennon, J. T., Martiny, J. B. H., Matulich, K. L., Schmidt, T. M., & Handelsman,

J. (2012). Fundamentals of microbial community resistance and resilience. *Frontiers in Microbiology*, **3**. https://doi.org/10.3389/fmicb.2012.00417

Song, K., Xie, G.-J., Qian, J., Bond, P. L., Wang, D., Zhou, B., Liu, Y., & Wang, Q. (2017). Improved degradation of anaerobically digested sludge during post aerobic digestion using ultrasonic pretreatment. *Environmental Science: Water Research & Technology*, **3**(5), 857– 864. https://doi.org/10.1039/C7EW00051K

Stackebrandt, E., & Goodfellow, M. (1991). *Nucleic acid techniques in bacterial systematics*. Wiley.

Sui, Q., Jiang, L., Di, F., Yue, W., Chen, Y., Wang, H., Chen, M., & Wei, Y. (2020). Multiple strategies for maintaining stable partial nitritation of low-strength ammonia wastewater. *Science of the Total Environment*, **742**, 140542. https://doi.org/10.1016/j.scitotenv.2020.140542

Tomei, M. C., Carozza, N. A., & Mosca Angelucci, D. (2016). Post-aerobic digestion of waste sludge: Performance analysis and modelling of nitrogen fate under alternating aeration. *International journal of Environmental Science and Technology*, **13**, 21– 30. https://doi.org/10.1007/s13762-015-0839-5

Tomei, M. C., Rita, S., & Mininni, G. (2011). Performance of sequential anaerobic/aerobic digestion applied to municipal sewage sludge. *Journal of Environmental Management*, **92**(7), 1867– 1873. https://doi.org/10.1016/j.jenvman.2011.03.016

Tong, Y., Mayer, B. K., & McNamara, P. J. (2016). Triclosan adsorption using wastewater biosolids-derived biochar. *Environmental Science: Water Research & Technology*, **2**(4), 761– 768. https://doi.org/10.1039/C6EW00127K

Tong, Y., McNamara, P. J., & Mayer, B. K. (2017). Fate and impacts of triclosan, sulfamethoxazole, and 17β-estradiol during nutrient recovery via ion exchange and struvite precipitation. *Environmental Science: Water Research & Technology*, **3**(6), 1109– 1119. https://doi.org/10.1039/C7EW00280G

Vadivelu, V. M., Keller, J., & Yuan, Z. (2007). Effect of free ammonia on the respiration and growth processes of an enriched Nitrobacter culture. *Water Research*, **41**, 826– 834. https://doi.org/10.1016/j.watres.2006.11.030

Vázquez-Padín, J. R., Fernández, I., Morales, N., Campos, J. L., Mosquera-Corral, A., & Méndez, R. (2011). Autotrophic nitrogen removal at low temperature. *Water Science and Technology*, **63**, 1282– 1288. https://doi.org/10.2166/wst.2011.370

Venkiteshwaran, K., McNamara, P. J., & Mayer, B. K. (2018). Meta-analysis of non-reactive phosphorus in water, wastewater, and sludge, and strategies to convert it for enhanced phosphorus removal and recovery. *Science of the Total Environment*, **644**, 661– 674. https://doi.org/10.1016/j.scitotenv.2018.06.369

Wang, L., Qiu, S., Guo, J., & Ge, S. (2021). Light irradiation enables rapid start-up of Nitritation through suppressing nxrB gene expression and stimulating Ammonia-oxidizing Bacteria. *Environmental Science & Technology*, **55**(19) 13297–13305. https://doi.org/10.1021/acs.est.1c04174

Wang, Q., Zhou, X., Peng, L., Wang, D.-B., Xie, G.-j., & Yuan, Z. (2016). Enhancing post aerobic digestion of full-scale anaerobically digested sludge using free nitrous acid pretreatment. *Chemosphere*, **150**, 152– 158. https://doi.org/10.1016/j.chemosphere.2016.02.035

Wei, W., Zhou, X., Wang, D., Sun, J., Nghiem, L. D., & Wang, Q. (2018). Free Ammonia pretreatment to enhance biodegradation of anaerobically digested sludge in post aerobic digestion. *ACS Sustainable Chemistry & Engineering*, **6**(9), 11836– 11842. https://doi.org/10.1021/acssuschemeng.8b02125

Wickham, H. (2011). ggplot2. *Wiley Interdisciplinary Reviews: Computational Statistics*, **3**, 180– 185. https://doi.org/10.1002/wics.147

Wickham, H., François, R. (2014) dplyr: A grammar of data manipulation.

Winkler, M. K., Bassin, J. P., Kleerebezem, R., Sorokin, D. Y., & van Loosdrecht, M. C. (2012). Unravelling the reasons for disproportion in the ratio of AOB and NOB in aerobic granular sludge. *Applied Microbiology and Biotechnology*, **94**(6), 1657– 1666. https://doi.org/10.1007/s00253-012-4126-9

Ye, L., & Zhang, T. (2011). Ammonia-oxidizing bacteria dominates over ammonia-oxidizing archaea in a saline nitrification reactor under low DO and high nitrogen loading. *Biotechnology and Bioengineering*, **108**(11), 2544– 2552. https://doi.org/10.1002/bit.23211

Yilmaz, P., Parfrey, L. W., Yarza, P., Gerken, J., Pruesse, E., Quast, C., Schweer, T., Peplies, J., Ludwig, W., & Glöckner, F. O. (2014). The SILVA and "all-species living tree project (LTP)" taxonomic frameworks. *Nucleic Acids Research*, **42**(D1), D643– D648. https://doi.org/10.1093/nar/gkt1209

Yu, M., Su, W.-Q., Huang, L., Parikh, S. J., Tang, C., Dahlgren, R. A., & Xu, J. (2021). Bacterial community structure and putative nitrogen-cycling functional traits along a charosphere gradient under waterlogged conditions. *Soil Biology and Biochemistry*, **162**, 108420. https://doi.org/10.1016/j.soilbio.2021.108420

Zhang, Y., Wang, S., Gu, S., Zhang, L., Dong, Y., Jiang, L., Fan, W., & Peng, Y. (2021). The combined effects of biomass and temperature on maximum specific ammonia oxidation rate in domestic wastewater treatment. *Frontiers of Environmental Science & Engineering*, **15**(6), 123. https://doi.org/10.1007/s11783-021-1411-9

Zhang, F., Yang, H., Wang, J., Liu, Z., & Guan, Q. (2018). Effect of free ammonia inhibition on NOB activity in high nitrifying performance of sludge. *RSC Advances*, **8**(56), 31987– 31995. https://doi.org/10.1039/C8RA06198J

Zheng, X., Zhou, W., Wan, R., Luo, J., Su, Y., Huang, H., & Chen, Y. (2018). Increasing municipal wastewater BNR by using the preferred carbon source derived from kitchen wastewater to enhance phosphorus uptake and short-cut nitrification-denitrification. *Chemical Engineering Journal*, **344**, 556– 564. https://doi.org/10.1016/j.cej.2018.03.124

Zhou, Z., Qi, M., & Wang, H. (2020). Achieving partial nitrification via intermittent aeration in SBR and short-term effects of different C/N ratios on reactor performance and microbial community structure. *Water*, **12**, 3485. https://doi.org/10.3390/w12123485

Zupančič, G. D., & Roš, M. (2008). Aerobic and two-stage anaerobic–aerobic sludge digestion with pure oxygen and air aeration. *Bioresource Technology*, **99**, 100– 109. https://doi.org/10.1016/j.biortech.2006.11.054